DOI 10.5012/bkcs.2010.31.7.1981

Characterization and Photonic Effect of Novel Ag-CNT/TiO_2 Composites and their Bactericidal Activities

Feng-Jun Zhang[†,‡] **and Won-Chun Oh**[‡,*]

[†]*School of Materials and Chemical Engineering, Anhui University of Architecture, Anhui Hefei 230022, P. R. China*
[‡]*Department of Advanced Materials & Science Engineering, Hanseo University, Seosan, Chungnam 356-706, Korea*
[*]*E-mail: wc_oh@hanseo.ac.kr*
Received February 26, 2010, Accepted May 23, 2010

A novel composite (Ag-CNT/TiO_2) of silver treated carbon nanotubes (Ag-CNT) and TiO_2 was synthesized *via* wet chemistry followed by a heat treatment. The dispersion and structure of the silver in the synthesized composites determined by X-ray diffraction (XRD), energy dispersive X-ray (EDX) spectroscopy, scanning electron microscopy (SEM), and transmission electron microscopy(TEM). XRD patterns of the composites showed that the composites contained a mixing anatase and rutile phase. The EDX spectra showed the presence of C, O, Ti and Ag peaks. The TiO_2 particles were distributed uniformly in the CNT network, and silver particles were virtually fixed on the surface of the tube. The photocatalysis degraded behaviors of the Ag-CNT/TiO_2 composites of the methylene blue, which increased with an increase of the silver component. The Ag-CNT/TiO_2 composites have excellent antibacterial activities against *Escherichia coli (E. Coli)*, *Pseudomonas aeruginosa* (*P. Aeru*) and *Bacillus subtilis* (*B. Sub*) under visible light.

Key Words: Sliver, CNT, TiO_2, Photocatalysis, Bactericidal activity

Introduction

Due to the widespread use of antibiotics, the resistance of bacteria to bactericides and antibiotics bacterial has increased gradually in recent years. Spores have no metabolism and can withstand a wide range of environmental assaults including heat, UV and solvents.[1-3] Moreover, some antimicrobial agents are extremely irritant and toxic, and there is much interest in finding ways to formulate new types of safe and cost-effective biocidal materials.

In general, the most effective way for inactivation to be achieved is to use highly efficient photocatalysts with UV illumination. Titania (TiO_2) is an important semiconducting material that is applied in photcatalytic and photosensitive active materials because of its excellent physical and chemical properties. The wide band-gap semiconductors often act as sensitizers for light-induced redox processes due to their electronic structure, which is characterized by a filled valence band and an empty conduction band.[4] Hydroxyl radicals (OH•) generated by the TiO_2 photocatalyst are very potent oxidants and are nonselective in reactivity.[5,6] When irradiated, TiO_2 particles are in direct contact with or close to microbes, hence the microbial surface becomes the primary target of the initial oxidative attack.

Recently, porous carbon materials have been widely used in waste water treatment to remove various pollutants, as a result of their large surface area and high adsorption capacity. Carbon based TiO_2 composites have attracted much attention and have become a very active field of research due to their unique properties and promising applications in pollution management.[7-12] In particular, Fullerenes and carbon nanotubes (CNT) have attracted considerable attention of late, as a result of their remarkable photoelectrical and mechanical properties, in addition to their other composites that possess intrinsic properties as materials exhibiting cooperative and/or synergetic effects.[13-15] Current synthesis and characterization of these nanomaterials can yield much more advanced colloidal photocatalytic nanoparticulate systems, which will allow enhanced photocatalytic activities. When TiO_2 is coated on the CNT, the combination of large specific surface area will increase, binding to bacteria and viruses. Where the electron-hole recombination is retarded by electron trapping at the TiO_2-CNT interfaces, the specific electronic properties of the composites (TiO_2/CNT), will yield a superior photocatalyst.[16-20] The proximity of the chemical reactants due to adsorption plus the increased number of hydroxyl radicals, which are the main cause for sterilization, can now be maximized.

Silver is traditionally made up of well-known antimicrobial materials. Silver ions have been found to have antibacterial effects on some microbes. Several studies have demonstrated that silver ions are selectively toxic, affecting only prokaryotic microorganisms, and having little effect on eukaryotic cells.[21] In the past decade, for the sake of safety, an inorganic antibacterial method, such as doping silver or copper to the alloy, has replaced the organic methods. Metallic ions from the alloy can penetrate the wall and membrane of bacterial cells and inhibit their breeding. In order to enhance antibacterial property, some silver implanted carbon composites were used, and these have been reported in the references.[22-27] When these metals are prepared in the form of very small particles, they are expected to show better antimicrobial characteristics because of their larger specific surface area.

In this study, the Ag-CNT/TiO_2 composites were put forward in a bactericidal application under visible light. Structural variations, surface state, and elemental compositions were investigated by preparation of the Ag-CNT/TiO_2 composites. XRD, EDX, SEM and TEM techiques were employed for characterization of these new photocatalysts. The catalytic efficiency of the Ag-CNT/TiO_2 composites was evaluated by the photocatalytic de-

gradation of methylene blue (MB, $C_{16}H_{18}N_3S{\cdot}Cl{\cdot}3H_2O$). Then the bactericidal property of Ag-CNT/TiO_2 was evaluated by halo test with bacteria of *E. Coli*, *P. Aeru* and *B. Sub*.

Experimental

Materials. CNT were selected as the support material. The CNT supplied from Carbon Nano-Material Technology Co., Ltd, Korea (Multiwall nanotubes, diameter: ~20 nm, length: ~5 μm) was used without further purification. The TNB (Ti (OC_4H_7)$_4$) as a titanium source for the preparation of composites was purchased from Acros Organics, New Jersey, USA. For the oxidization of the surface of the CNT, *m*-chloroperbenzoic acid (MCPBA) was used as an oxidized reagent; also purchased from Acros Organics, New Jersey, USA. MB was the analytical grade chemical used; purchased from Duksan Pure Chemical Co., Ltd, Korea. Benzene (99.5%) was used as an organic solvent which was purchased from Samchun Pure Chemical Co., Ltd, Korea. Silver nitrate ($AgNO_3$) was obtained from Duksan Pure Chemical Co., Ltd, Korea. Reagent-grade solvents, benzene and ethyl alcohol, were purchased from Duksan Pure Chemical Co. and Daejung Chemical Co., Korea and were used without further purification unless otherwise stated. *E. Coli*, *P. Aeru* and *B. Sub* used standard test strains.

Preparation of Ag-CNT composites. For preparing the oxidizing agent, 2.0 g MCPBA was melted in 60 mL Benzene. Then 0.6 g CNT was put into the oxidizing agent, refluxed for 6 h, filtered and dried. The oxidized CNT was put into the different concentrations of silver nitrate solutions, and then the solutions were homogenized under reflux at 343 K for 2 h using a magnetic stirrer in a vial. After being heat treated at 373 K for 1 h, the Ag treated CNT composites were obtained.

Preparation of Ag-CNT/TiO_2 composites. The Ag treated CNT composites were put into the mixing solution of TNB and Benzene with a volume ratio of 4:16. Then the solutions were homogenized under reflux at 343 K for 5 h, while being stirred in a vial again. Having been stirred, the solutions transformed into Ag-CNT/TiO_2 gels, and these gels were heat treated at 973 K for 1 h with a heating rate of 279 K/min. After cooling, the Ag-CNT/TiO_2 composites were resulted. The preparation condition and sample codes are listed in Table 1.

Characterization of the Ag-CNT/TiO_2 composites. XRD technique was used for crystal phase identification and estimation of the anastase-to-rutile ratio. XRD patterns were obtained at room temperature with a diffractometer Shimata XD-D1 (Japan) using Cu Kα radiation. SEM was used to observe the surface state and porous structure of the Ag-CNT/TiO_2 composites using a scanning electron microscope (JOEL, JSM-5200, Japan). EDX spectroscopy was used to measure the elemental analysis of the Ag-CNT/TiO_2 composites. TEM (JEOL, JEM-2010, Japan) at an acceleration voltage of 200kV was used to investigate the size and distribution of the silver and titanium deposits on the CNT surface of various samples. TEM specimens were prepared by placing a few drops of the sample solution on a carbon grid.

Analysis of photocatalytic effect. In order to analyze the photocatalytic effect, the decomposition reaction of MB in water was followed. Prior to illumination, powdered samples of 0.05 g were dispersed in the MB solution under ultra sonicate and impregnated in the pristine MB solution in the dark for 30 min needed to achieve adsorption/desorption equilibrium. For irradiation, a UV lamp (20 W, 365 nm) or visible light (8W, KLD-08L/P/N, FAWOO TECHNOLOGY), were used at a distance of 100 mm from the solution in the dark box. The suspension was irradiated with UV light or visible light as a function of irradiation time. Samples were then withdrawn regularly from the reactor and powders were dispersed through centrifuge. The clean transparent solution was analyzed by UV-vis spectroscopy. The concentration of MB in the solution was determined as a function of irradiation time.

Bactericidal test. For the bactericidal effects, three kinds of bactericidal materials were used: the standard *ampicillin* (*Amp.*) and *teracyclin* (*Tc*) as antibiotics and the Ag-CNT/TiO_2 composites as bactericides. Employing the halo test proposed by the Berman method,[28] the bactericidal activities against *E. Coli*, *P. Aeru* and *B. Sub* were examined in a cultivated culture medium.

Results and Discussion

Structure and morphology of CNT/ TiO_2 composites. The XRD results for the catalyst samples are shown in Fig. 1. Diffraction peaks corresponding to the anatase and rutile phases have been marked with 'A' and 'R', respectively. Diffraction peaks corresponding to sliver-3C phases have been marked with 'S'.

The structures of the Ag-CNT/TiO_2 composites showed a mix of anatase and rutile crystals. It is well known that the crystal structure of the titanium dioxide is mainly determined by the heat treated temperature. The peaks at 25.3, 37.8, 48.0 and 62.5^o are the diffractions of (101), (004), (200) and (204) planes of anatase, indicating the developed Ag-CNT/TiO_2 composites existed in an anatase state. The peaks at 27.4, 36.1, 41.2 and 54.3^o belong to the diffraction peaks of (110), (101), (111) and (211) of rutile. Therefore, it can be concluded that the developed CNT/TiO_2 composites had a mixing structure of anatase and rutile crystals when annealed at 973K. According to the published paper, if the anatase phase is formed below 773 K, it starts to transformed into a rutile-type structure above 873 K, and then

Table 1. Nomenclatures of Ag-CNT/TiO_2 composites

Preparation method	Nomenclatures
2.0 g MCPBA + 0.6 g CNT + $AgNO_3$ (0.02 M) + (TNB 4 mL + benzene 16 mL)	ACT1
2.0 g MCPBA + 0.6 g CNT + $AgNO_3$ (0.04 M) + (TNB 4 mL + benzene 16 mL)	ACT2
2.0 g MCPBA + 0.6 g CNT + $AgNO_3$ (0.06 M) + (TNB 4 mL + benzene 16 mL)	ACT3
2.0 g MCPBA + 0.6 g CNT + $AgNO_3$ (0.08 M) + (TNB 4 mL + benzene 16 mL)	ACT4

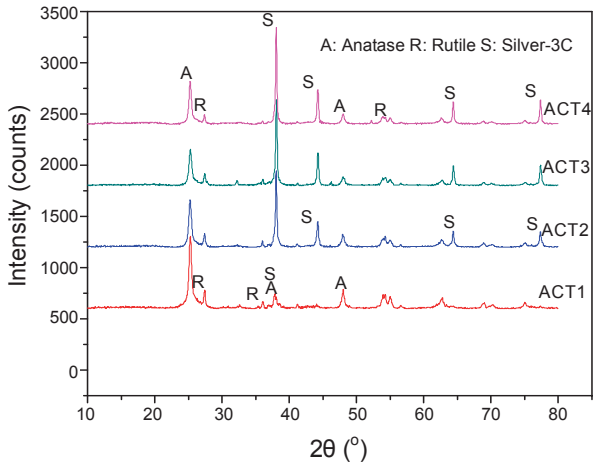

Figure 1. XRD patterns of Ag-CNT/TiO_2 composites.

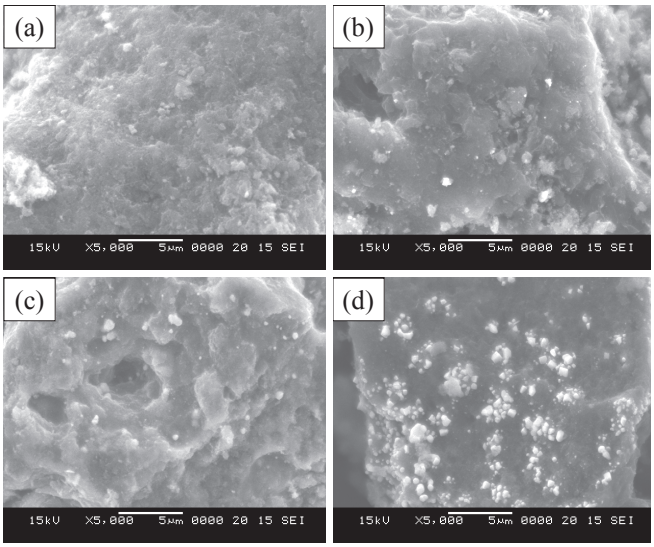

Figure 2. SEM images obtained from powdered Ag-CNT/TiO_2 composites: (a)ACT1, (b) ACT2, (c) ACT3, (d) ACT4.

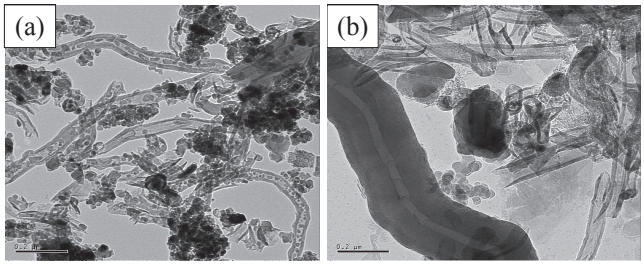

Figure 3. TEM micrograph of (a) CNT/TiO_2 composite and (b) Ag-CNT/TiO_2 composite.

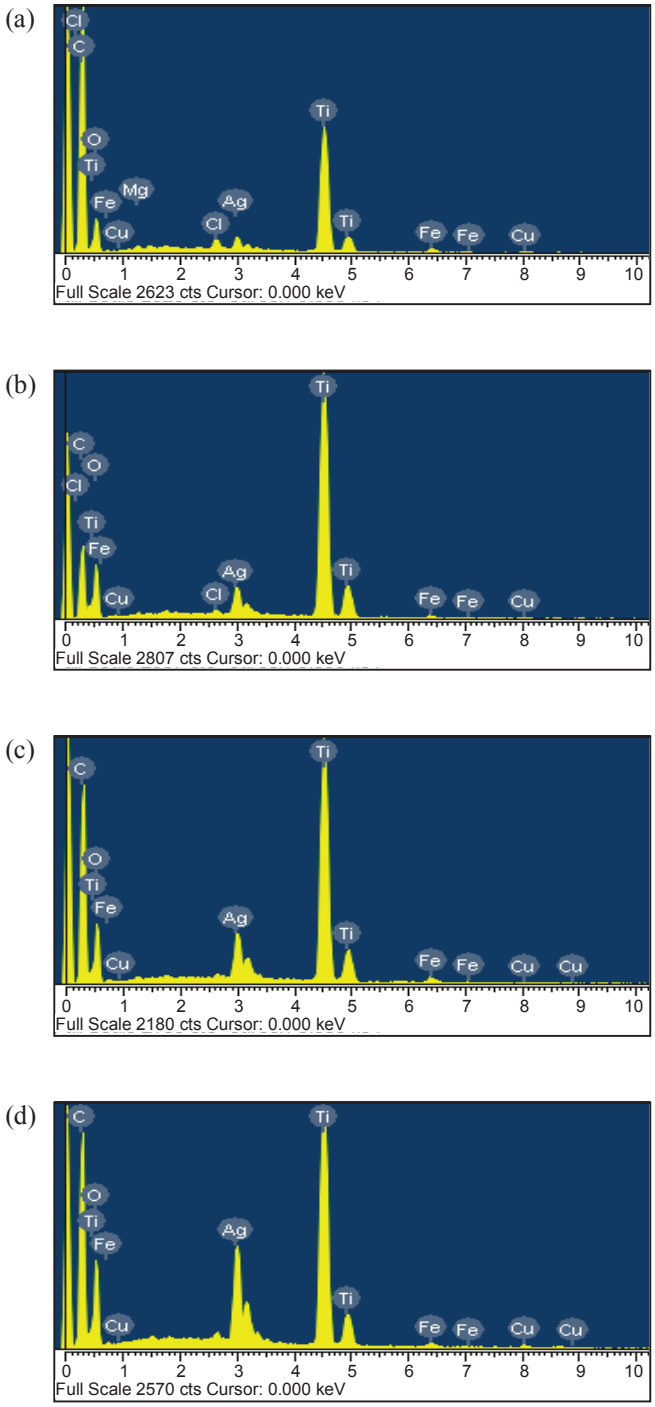

Figure 4. EDX elemental microanalysis of Ag-CNT/TiO_2 composites:(a) ACT1, (b) ACT2, (c) ACT3, (d) ACT4.

changes into a single phase of rutile at 973 K ~ 1173 K.[29] We have previously demonstrated that the crystallization phenomena in C/TiO_2 composites that are heat treated at 973K results in a mixed anatase-rutile structure.[11,30] Thus The XRD result obtained here is reasonable.

In addition, the peaks denoting the silver component have been observed in the Ag-CNT/TiO_2 samples. The peaks at 38.18, 44.39, 64.58, and 77.54° are assigned as the (111), (200), (220), and (311) reflection lines of fcc Ag particles (JCPDS file, No. 04-0783), respectively.[21,31] Intense peaks from Ag metal appeared in the Ag-CNT/TiO_2 and became stronger with increasing concentration of the $AgNO_3$ solution. Sharp diffraction peaks indicated the formation of pure silver of high crystalline.

The micro-surface structures and morphology of the Ag-CNT/TiO_2 composites were characterized by SEM (Fig. 2) and TEM (Fig. 3). Fig. 2 shows the macroscopical changes in the

Table 2. EDX elemental microanalysis of Ag-CNT/TiO_2 composites

Sample	C	O	Ti	Ag
ACT1	55.70	20.96	18.29	2.47
ACT2	40.99	30.99	21.04	5.40
ACT3	36.24	29.64	26.57	6.67
ACT4	31.46	33.28	22.40	11.65

morphology of the Ag-CNT/TiO_2 composites. As shown in Fig. 2, the TiO_2 particles were well attached to the surface of the CNT network, and the distribution was uniform. According to Wang's reports,[9] a good dispersion of small particles could provide more reactive sites for the reactants than aggregated particles. At the same time, the conductive of the CNT network can facilitate the electron transfer between the adsorbed dyes molecules and the catalyst substrate.[32] It was beneficial for the enhancement of the photocatalytic activity of these composites. Moreover, silver particles were fixed on the surface of the CNT network in small clusters, and the distribution was not uniform. Moreover, the amount of agglomerated silver particles results in the increase of the Ag content. These particles were heavily agglomerated to form lager clusters (Fig. 2(d)), and these results can be seen clearly in Fig. 2(a) to Fig. 2(d). These results are also confirmed by TEM inspection of the Ag-CNT/TiO_2 composites. As shown in Fig. 3(a), the TiO_2 particles distributed uniformly inside and on the surface of the CNT for the CNT/TiO_2 composites. However, the inside of the CNT is almost empty of the Ag-CNT/TiO_2 composites. In most cases, Ag particles were formed inside the tubes due to the capillary effect,[33,34] leading to poor synergic effect of the Ag-CNT composites. As shown in Fig. 3(b), for the Ag-CNT/TiO_2 composites, silver particles were roughly almost fixed on the surface of the tube, although this caused partial agglomeration. The TiO_2 particles were still distributed uniformly in the CNT network.

Fig. 4 shows the EDX spectra of Ag-CNT/TiO_2 composites prepared. From the EDX data, the main elements such as C, O, Ti and Ag existed, and other impure elements also existed. The results of the EDX elemental microanalysis of the CNT/TiO_2 composites are listed in Table 2. The contents of the silver component for ACT1, ACT2, ACT3 and ACT4 are 2.47, 5.40, 6.67 and 11.65%, respectively. It can be expected that the contents of the silver component in the composites increased with an increase of $AgNO_3$ concentration. It was proposed that the increase of the Ag content increased the amount of the agglomerated silver particles. The same phenomena can be observed in the micro-surface structures and morphology of Ag-CNT/TiO_2 composites (Fig. 2).

Photocatalytic decomposition of MB. From the results of UV-vis spectra for the MB solution after photolysis, we attempted to compare of the relative yields of the photoproducts formed at various functions of irradiation time. The UV-vis spectra of MB concentration against the Ag-CNT/TiO_2 composite derivatives under various time conditions are shown in Fig. 5. Here we discussed three kinds of degradation process: 1). Dark adsorption; 2). UV light irradiation; 3).Visible light irradiation. The difference of dark adsorption in 30 min for all samples is not clear. As shown in Fig. 5(a), we can observe that the photo

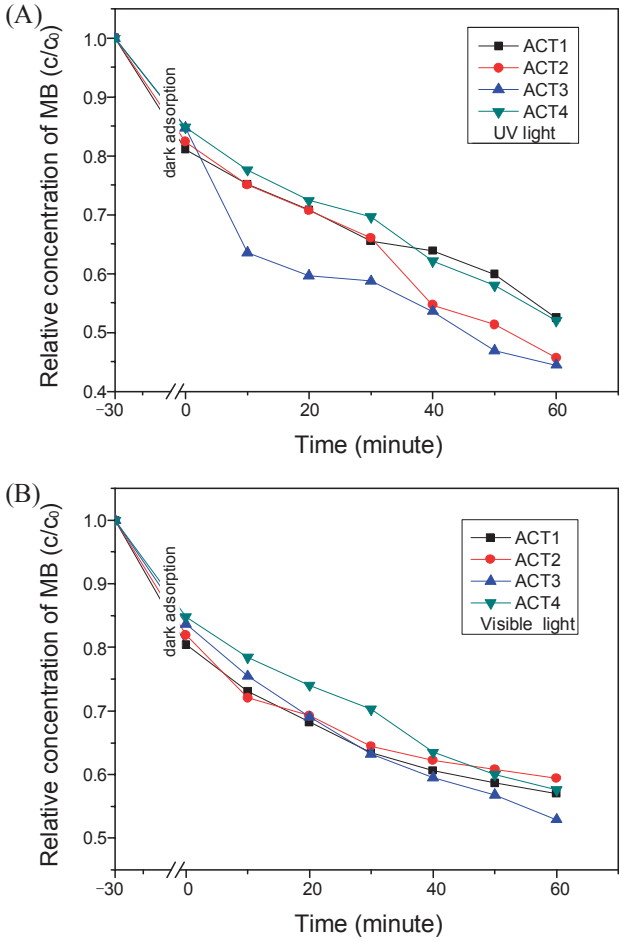

Figure 5. Dependence of the relative concentration (c/c_0) of MB solution for different Ag-CNT/TiO_2 composites on irradiation time of UV light (a) and visible light (b).

catalytic (PC) degradation efficiency of the sample ACT3 is higher than that of the samples ACT1, ACT2 and ACT4 in the same irradiation time. According to the former studies,[16,17] the Ti content of ACT3 is highest among the four samples; we can consider that the ACT3 will have better PC degradation of MB solution than that of the other samples. As a result of the EDX, among the four kinds of Ag-CNT/TiO_2 composites, the ACT3 has the lowest content of carbon and the highest content of Ti. It is considered that a decrease of MB concentration in the aqueous solution can occur in two physical phenomena: adsorption by CNT and PC decomposition by TiO_2. It was possible that the CNT/TiO_2 composites catalytic decomposition of the MB solution could be attributed to the effects of combining between PC oxidation of TiO_2 and electro-assistant of the CNT. In this study, we also found that the ACT4 had worse PC degradation of MB solution than that of the other samples, although it contains the highest content of silver. It is probable that the PC activity is seriously affected by the content and morphology of the silver particles in the Ag-CNT/TiO_2 composites. Comparison with the Fig. 5(a) and (b), the PC effects of the Ag-CNT/TiO_2 composites were all better under UV light than that of visible light in the irradiation time of 60 minutes. It is well known that it can be more easily excited under UV light than visible light because

of the large band gap for anatase TiO_2. However, at the irradiation time of 60 min, the relative concentration value of MB solution for different Ag-CNT/TiO_2 composites under visible light arrived at 52.7 - 59.4%. It can be observed that the PC activity will increase with the increase of silver content in a certain range. At the same time, the morphology of silver in the Ag-CNT/TiO_2 composites is an important factor. The optimization of PC oxidation of MB using Ag-CNT/TiO_2 composites will be studied in detail in another paper.

Antibacterial activity. The antibacterial activities against *E.Coli*, *P.Aeru* and *B.Sub* were investigated. For the comparison, we choose the standard antibiotics (*Amp*. and *Tc*) and the Ag-CNT/TiO_2 composites as the bactericides. The three kinds of bacterias are incubated in a culture media containing these antibiotics and bactericides. Fig. 6 ((a1), (a2) and (a3)) shows the results on the *Amp., Tc* and Ag-CNT/TiO_2 composites against *E. Coli*. In the case of the Amp, Tc and Ag-CNT/TiO_2 composites, the clear zones near all of antibiotics and bactericides formed at the same conditions. In particular, the clear zone of Ag-CNT/TiO_2 named as ACT3 is the largest one. These results obviously indicate that the *Amp.*, *Tc* and Ag-CNT/TiO_2 present excellent antibacterial activity against *E. Coli*. Moreover, out of the two antibiotics and the four bactericides, the Ag-CNT/TiO_2 named as ACT3 has the strongest antibacterial activity against *E. Coli* for the Ag-CNT/TiO_2 series. In addition, the antibacterial activities against *E. Coli* using the ACT3 and ACT2 in the Ag-CNT/TiO_2 composite series are better than that of the ACT1 and ACT4. It was probable that the antibacterial activity is affected by the content and morphology of silver in the Ag-CNT/TiO_2 composites. It is well known that the antibacterial activity will increase with the increase of silver content. At the same time, the size and dispersion state of silver particles in the Ag-CNT/TiO_2 composites is an important factor. For the ACT4 of Ag-CNT/ TiO_2, the silver particles were highly agglomerated to form lager clusters (Fig. 2(d)).

Fig. 6 ((b1), (b2) and (b3)) shows the results on the *Amp*., *Tc* and Ag-CNT/TiO_2 composites against *P. Aeru*. In the case of the *Amp.* and *Tc*, the zones near all of antibiotics not become clear. However, for the Ag-CNT/TiO_2, the zones near all of Ag-CNT/TiO_2 bactericides become clear at the same conditions. The clear zone of Ag-CNT/TiO_2 named as ACT3 is also the largest one against *P. Aeru*. These results obviously indicate that the *Amp.*, *Tc* have no the antibacterial activity against *P. Aeru*, while the prepared Ag-CNT/TiO_2 possess strong antibacterial activity against *P. Aeru*. In all of the Ag-CNT/TiO_2 bactericides, Ag-CNT/TiO_2 named as ACT3 has the strongest antibacterial activity against *P. Aeru.*

Fig. 6 ((c1), (c2) and (c3)) shows the results on the *Amp.*, *Tc* and Ag-CNT/TiO_2 composites against *B. Sub*. The zones near *Amp.* are not very clear. In contrast, the zones near *Tc* and Ag-CNT/TiO_2, all become clear at the same conditions. The clear zone of Ag-CNT/TiO_2 named as ACT3 is also the largest one against *B. Sub*. These results obviously indicate that the *Amp.* does not have the antibacterial activity against *B. Sub*, while *Tc* and the prepared Ag-CNT/TiO_2 possess strong antibacterial activity against *B. Sub*. Moreover, in all of *Tc* and the prepared Ag-CNT/TiO_2 bactericides, the Ag-CNT/TiO_2 named as ACT3 has the strongest antibacterial activity against *B.sub*.

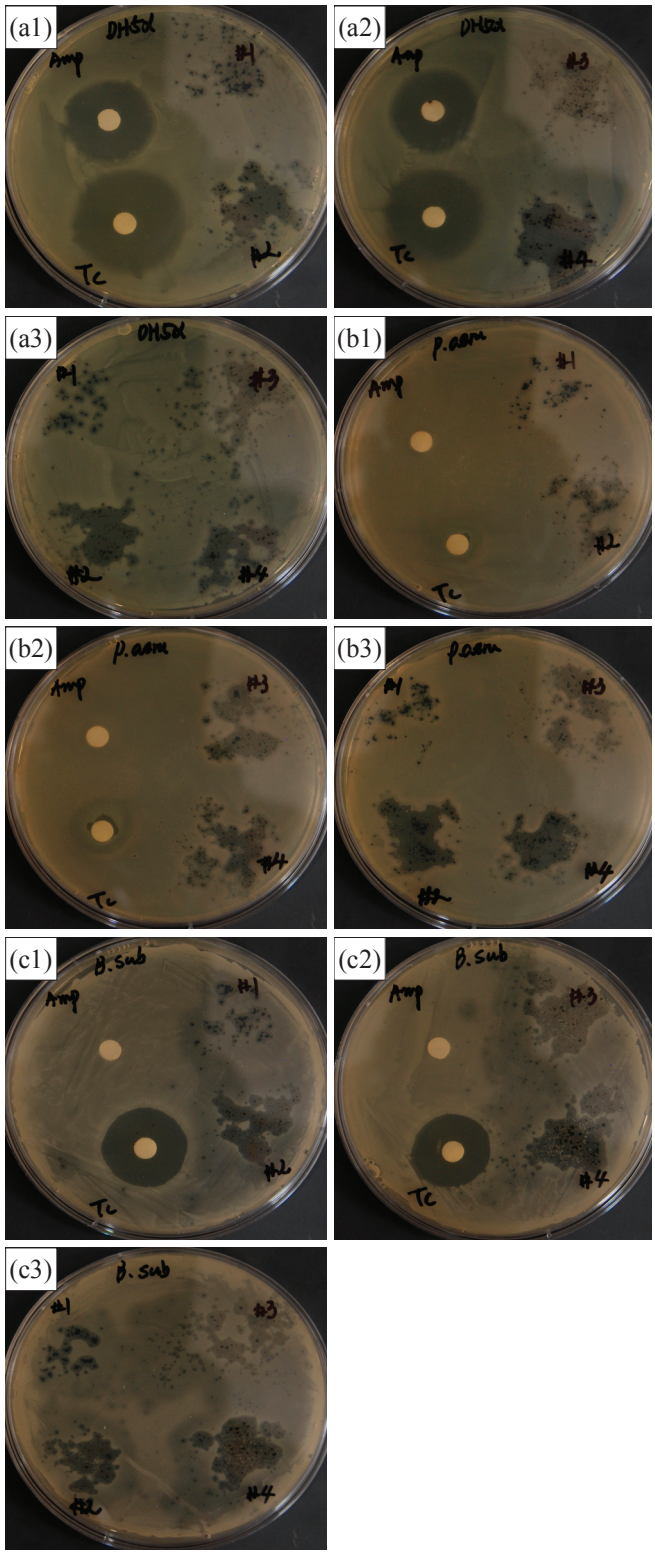

Figure 6. Photographs of bactericidal effects by halo test for different bacterias with standard bactericides (*ampicillin* (*Amp*) and *teracyclin* (*Tc*)) and the Ag-CNT/TiO_2 composites (ACT1: #1; ACT2: #2; ACT3: #3; ACT4: #4): (a1), (a2), (a3) *Escherichia Coli* DH-52(DH52).

To quantify the antimicrobial results, the changes in the residual amount of strains used were shown in Fig. 7. Antibacterial activity of the Ag-CNT/TiO_2 sample was judged by counting

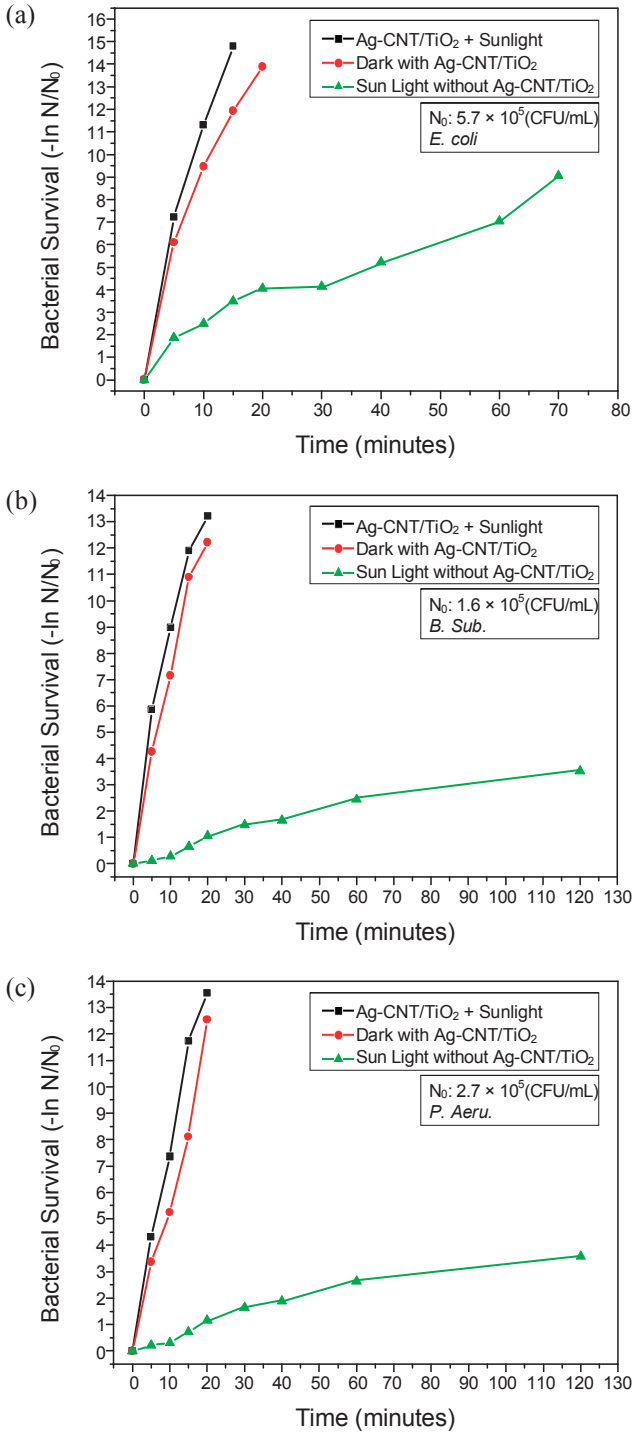

Figure 7. Effects of Ag-CNT/TiO_2 composites on (*E. coli* (a), *B.sub* (b) and *P.aeru* (c)) survival with or without sunlight as a function of time.

the number of each strain. The direct germicidal action of sunlight with or without the addition of Ag-CNT/TiO_2 composite is presented in Fig. 7. The total time of bacterial abatement was shorter in the presence of Ag-CNT/TiO_2 composites than without almost for different bacteria (*E. Coli*, *P. Aeru* and *B. Sub*). Based on the bacterial survival number, the graph of -ln (N/N_0) *versus* time should give a straight line, where: N represents the bacterial survival number at time (t); N_0, the initial number of bacteria; and t, the contact time. As shown in Fig. 7, it can be seen from the curves that inactivations of the *E. Coli*, *P. Aeru* and *B. Sub* were much more effective for the Ag-CNT/TiO_2 composite under sunlight or dark condition than in experimental case without Ag-CNT/TiO_2 composite. The antibacterial effects with Ag-CNT/TiO_2 appeared after a very short contact time between the cells and the Ag-CNT/TiO_2 under sunlight. The application of a promising route for destroying bacteria can be founded upon the basic principles and studies reported in the literature.[35,36] As confirmed by bactericidal tests, the Ag-CNT/TiO_2 showed microbicidal effects and strong antibacterial activity against the strain used. Solar disinfection with Ag-CNT/TiO_2 composites is a consequence of both the direct action of the light on the microorganisms and the photocatalytic action of the photo-induced electron (e^-) accepted by the CNT from the sunlight. It is regarded that the electrons in the CNT transfer into the conduction bands of the TiO_2 particles, resulting primarily from absorption by the deoxyribonucleic acid (DNA) of the microorganisms that yields a dimerization of the thymidine bases.

As a whole, the prepared Ag-CNT/TiO_2 bactericides have strong antibacterial activity against *E. Coli*, *P. Aeru* and *B. Sub* under visible light. Of the four kinds of Ag-CNT/TiO_2 bactericides, the antibacterial activity of ACT3 is the best. While the standard antibiotic *Amp.* has no antibacterial activity against *P. Aeru* and *B. Sub*, the *Tc* has no antibacterial activity against *P. Aeru*. From this perspective, this study has triumphantly prepared new kind of bactericides.

Conclusion

In this study, we present the fabrication and characterization of Ag-CNT/TiO_2 composite bactericides. XRD data revealed that the structure for the Ag-CNT/TiO_2 composites showed a mixing anatase and rutile crystals. The SEM and TEM microphotographs of Ag-CNT/TiO_2 composites showed that TiO_2 particles were distributed uniformly in the CNT network and the silver particles were fixed on the surface of the CNT, although they were partly aggregated. From the EDX data, the main elements such as C, O, Ti and Ag existed. Of the four samples of Ag-CNT/TiO_2 composites, the MB degradation efficiencies of the sample ACT3 had the best results. The prepared Ag-CNT/TiO_2 bactericides have strong antibacterial activity against *E. Coli*, *P.Aeru* and *B.Sub*. Of the four kinds of Ag-CNT/TiO_2 bactericides, the antibacterial activity of ACT3 is the best. While the standard antibiotic *Amp.* has no antibacterial activity against *P.Aeru* and *B. Sub*, the *Tc* has no antibacterial activity against *P.Aeru*.

Reference

1. Lee, S. H.; Pumprueg, S.; Moudgil, B.; Sigmund, W. *Colloid. Surf. B: Biointerfaces* **2005**, *40*, 93.
2. Sondi, I.; Sondi, B. S. *J. Colloid. Interface Sci.* **2004**, *275*, 177.
3. Atrih, A.; Foster, S. J. *Int. Dairy. J.* **2002**, *12*, 217.
4. Fujishima, A.; Honda, K. *Nature* **1972**, *238*, 37.
5. Hoffmann, M. R.; Martin, S. T.; Choi, W.; Bahnemann, D. W. *Chem. Rev.* **1995**, *95*, 69.
6. Linsebigler, A. L.; Lu, G.; Yates, J. T. *Chem. Rev.* **1995**, *95*, 735.
7. Zhang, Y.; Franklin, N. W.; Chen, R. J.; Dai, H. J. *Chem. Phys. Lett.*

2000, *331*, 35.
8. Fu, P. F.; Luan, Y.; Dai, X. G. *J. Mol. Catal. A: Chem*. **2004**, *221*, 81.
9. Wang, W. D.; Serp, P.; Kalck, P.; Faria, J. L. *J. Mol. Catal. A Chem*. **2005**, *235*, 194.
10. Chen, M. L.; Bae, J. S.; Oh, W. C. *Bull. Korean Chem. Soc*. **2006**, *27*, 1423.
11. Chen, M. L.; Bae, J. S.; Oh,W. C. *Carbon Sci*. **2006**, *7*, 259.
12. Ollis, D. F.; Alekabi, H. *Photcatalytic Purification and Treatment of Water and Air*; Elsevier: 1993; p 265.
13. Jitianu, A.; Cacciaguerra, T.; Benoit, R.; Delpeux, S.; Beguin, F.; Bonnamy, S. *Carbon* **2004**, *42*, 1147.
14. Phang, S. W.; Tadokoro, M.; Watanabe, J.; Kuramoto, N. *Synth. Metal.* **2008**, *158*, 251.
15. Ray, A. K. *Chem. Eng. Sci*. **1999**, *54*, 3113.
16. Oh, W. C.; Jung, A. R.; Ko, W. B. *J. Ind. Eng. Chem*. **2007**, *13*, 1208.
17. Oh, W. C.; Chen, M. L. *Bull. Korean Chem. Soc*. **2008**, *29*, 159.
18. Wang, W. D.; Serp, P.; Kalck, P.; Faria, J. L. *Appl. Catal. B: Environ*. **2005**, *56*, 305.
19. Oh, W. C.; Jung, A. R.; Ko, W. B. *Mater. Sci. Eng. C* **2008**, *29*, 1338.
20. Zhang, F. J.; Chen, M. L.; Oh, W. C. *Mater. Res. Soc. Korea* **2008**, *18*, 583.
21. Yoon, K. Y.; Byeon, J. H.; Park, J. H.; Hwang, J. H. *Sci. Total. Environ*. **2007**, *373*, 572.
22. Oh, W. C. *J. Ind. Eng. Chem*. **2003**, *9*, 117.
23. Oh, W. C. *Bull. Korean Chem. Soc*. **2004**, *25*, 639.
24. Liu, T.; Tang, H. Q.; Cai, X. M.; Zhao, J.; Li, D. J.; Li, R.; Sun, X. L. *Nucl. Inst. Meth. Phys. Res. B* **2007**, *264*, 282.
25. Zhang, S. T.; Fu, R. W.; Wu, D. C.; Xu, W.; Ye, Q. W.; Chen, Z. L. *Carbon* **2004**, *42*, 3209.
26. Park, S. J.; Jang, Y. S. *J. Colloid. Interface. Sci.* **2003**, *261*, 238.
27. Zhao, J.; Feng, H. J.; Tang, H. Q.; Zheng, J. H. *Nncl. Instr. Meth. B* **2006**, *243*, 299.
28. Berman, E. *Toxic Metals and Their Analysis*; Heyden and Son: London, 1980; p 116.
29. Inagaki, M.; Hirose,Y.; Matsunaga,T.; Tsumura,T.; Toyoda, M. *Carbon* **2003**, *41*, 2619.
30. Oh, W. C.; Chen, M. L. *J. Ceram. Process. Res.* **2008**, *9*, 100.
31. Powder Diffraction File, Joint Committee on Powder Diffraction Standards International Center for Diffraction Data, Swarthmore, PA, 1987, Card 04-0783.
32. Christensen, P. A.; Curtis, T. P.; Egerton, T. A.; Kosa, S. A. M.; Tinlin, J. R. *Appl. Catal. B: Environ.* **2003**, *41*, 371.
33. Ajayan, P. M.; Iijima, S. *Nature* **1996**, *361*, 333.
34. Ugarte, U.; Chatelain, A.; De Heer, W. A. *Science* **1996**, *274*, 1897.
35. Sunkara, B. K.; Misra, R. D. K. *Acta Biomaterialia* **2008**, *4*, 273.
36. Rana, S.; Rawat, J.; Sorensson, M. M. *Acta Biomaterialia* **2006**, *2*, 421.